

# Iron Nitride Clusters

DOI: 10.1002/ange.200601570

## Self-Assembly of a Tetradecanuclear Iron Nitride Cluster\*\*

Miriam V. Bennett and R. H. Holm\*

Recently, we reported the synthesis, structures, and certain electronic properties of the first examples of molecular mid-valent high-nuclearity iron nitride clusters.<sup>[1]</sup> Four clusters were obtained by self-assembly,  $[\text{Fe}_4\text{N}_2\text{Cl}_{10}]^{4-}$  (**1**),  $[\text{Fe}_{10}\text{N}_8\text{Cl}_{12}]^{5-}$  (**2**), and their bromide analogues (Scheme 1). This work was motivated in part by the revelation, from high-resolution protein crystallography, of a light atom X at the centre of the  $\text{Fe}_6$  portion of the  $\text{MoFe}_7\text{S}_9\text{X}$  cluster core in the iron–molybdenum cofactor (FeMoco) of nitrogenase.<sup>[2]</sup> Consideration of the electronic properties of the cofactor in three

[\*] Dr. M. V. Bennett, Prof. R. H. Holm  
Department of Chemistry and Chemical Biology  
Harvard University  
Cambridge, MA 02138 (USA)  
Fax: (+1) 617-496-9289  
E-mail: holm@chemistry.harvard.edu

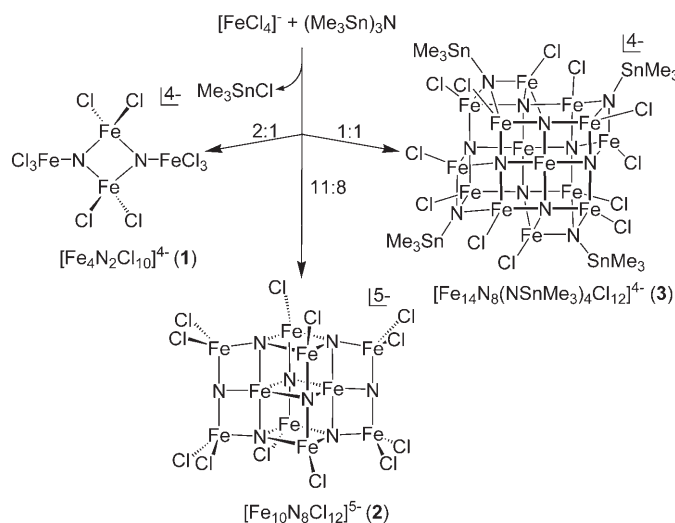
[\*\*] This research was supported by National Institutes of Health Grant GM 28856, and conducted in part at the Center for Materials Science and Engineering at M.I.T. M.V.B. is supported by a National Institutes of Health N.R.S.A. Fellowship.



Supporting information for this article is available on the WWW under <http://www.angewandte.org> or from the author.

oxidation states has led to the order of likelihood of  $N > O > C$  for the identity of atom X.<sup>[3]</sup> Subsequent electron nuclear double resonance (ENDOR) and electron spin echo envelope modulation (ESEEM) evidence has been interpreted as disfavoring nitrogen as atom X.<sup>[4]</sup> Shortly after the discovery of atom X, it was found that this atom does not exchange under enzyme turnover conditions with dinitrogen, suggesting that it serves a structural and/or electronic role in the cofactor.<sup>[4]</sup> In a chemical context, the presence of atom X requires that any synthesis of a cluster analogue of FeMoco incorporate atom X at some stage, and raises the possibility of a template effect in the construction of the cluster core.<sup>[5]</sup> Further, the presence of atom X implies the existence of a new class of clusters that possibly includes the generalized fragment  $Fe_n(\mu_n-X)$ .

We have pursued the exploratory synthesis of iron nitride clusters in a continuing attempt to disclose structures and structural principles that may be relevant to a synthetic analogue of FeMoco and its biosynthetic precursor(s). The desired clusters possess nuclearities exceeding two, differentiating them from various binuclear species with Fe-N-Fe bridges,<sup>[6–10]</sup> and are devoid of the carbonyl ligands present in interstitial low-valent clusters such as  $[Fe_5(\mu_5-N)(CO)_{14}]^{3-}$ <sup>[11]</sup> and  $[Fe_6(\mu_6-N)(CO)_{15}]^{3-}$ .<sup>[12]</sup> The cluster products in the assembly system of  $[FeCl_4]^-$  and  $(Me_3Sn)_3N$  in acetonitrile are primarily controlled by the molar ratio of the reactants (Scheme 1), although the reactant ratio is not necessarily



**Scheme 1.** Formation of clusters 1–3 in self-assembly systems with the indicated molar ratios of  $[FeCl_4]^-:(Me_3Sn)_3N$ .

expressed in the product composition. Clusters **1** and **2** were isolated as  $Et_4N^+$  salts at  $[FeCl_4]^-:(Me_3Sn)_3N$  ratios of 2:1 (72 % yield) and 11:8 (37 % yield).<sup>[1]</sup> Herein, a 1:1 stoichiometry affords the nitrido cluster  $[Fe_{14}N_8(NSnMe_3)_4Cl_{12}]^{4-}$  (**3**; 18 % yield), as well as two other clusters,  $[Fe_8N_2-(NSnMe_3)_6Cl_8]^{2-}$  and the prismane  $[Fe_6(NSnMe_3)_6Cl_6]^-$ , as highly air- and proton-sensitive  $Et_4N^+$  salts. The formation of these two additional clusters from the mother liquor containing **3** presumably contributes to the relatively low yield of **3**.

Cluster **3** contains several unique features (Figure 1).<sup>[13]</sup> Charge balance dictates a mixed-valent formulation of  $12Fe^{III} + 2Fe^{II}$ ; consequently, this is the first iron nitride cluster to contain ferrous ions. The cluster has crystallo-

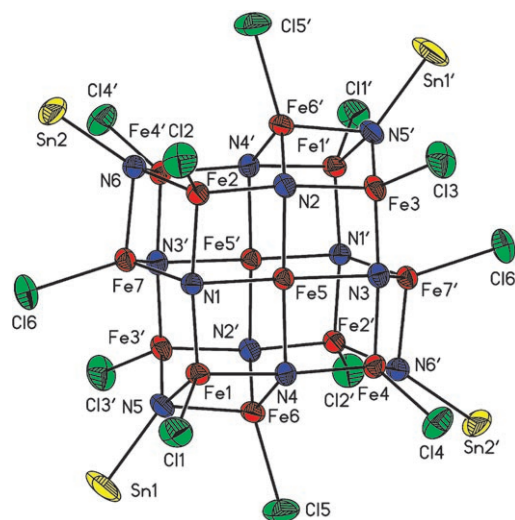


**Figure 1.** The structure of cluster **3**; thermal ellipsoids are set at 50 % probability; primed and unprimed atoms are related by an inversion center; methyl groups are omitted for clarity. Selected interatomic distances [Å] and angles [°]: Fe–Cl 2.239(8) ( $\angle$  of 6), Sn–N 2.100(2) ( $\angle$  of 2), Fe–( $\mu_3$ -N) 1.969(4) ( $\angle$  of 6), Fe–( $\mu_4$ -N) 1.902(12) ( $\angle$  of 12), Fe5...Fe5' 2.783(2), Fe5–( $\mu_4$ -N) 2.004(6) ( $\angle$  of 4); N–Fe5–N 89.6(3) ( $\angle$  of 4) and 171.0(2) ( $\angle$  of 2), Fe1,2–( $\mu_3$ -N)–Fe3',4' 117.4(4) ( $\angle$  of 2), Fe5–( $\mu_4$ -N)–Fe 119.3(6) ( $\angle$  of 4: Fe6–Fe7), Fe1–4–( $\mu_4$ -N)–Fe1–4 170(1) ( $\angle$  of 4), ( $\mu_3$ -N)–Fe–( $\mu_4$ -N) 114(1) ( $\angle$  of 4: Fe1–Fe4) 95.9(1) ( $\angle$  of 4: Fe1–Fe4), ( $\mu_4$ -N)–Fe–( $\mu_4$ -N) 95.9(6) ( $\angle$  of 4: Fe1–Fe4), ( $\mu_3$ -N)–Fe–( $\mu_4$ -N) 96.2(3) ( $\angle$  of 4: Fe6–Fe7), ( $\mu_4$ -N)–Fe–( $\mu_4$ -N) 109.0(4) ( $\angle$  of 4: Fe6–Fe7), Sn–( $\mu_3$ -N)–Fe 120(2) ( $\angle$  of 6). In an interior rhomb (Fe1N1Fe5N4): Fe1–N1 1.893(5), Fe1–N4 1.918(5), Fe5–N1 2.003(5), Fe5–N4 2.001(5), Fe1...Fe5 2.694(1), N1...N4 2.829(2); N1–Fe1–N4 95.8(2), N1–Fe5–N4 89.9(2), Fe1–N1–Fe5 87.4(2), Fe1–N4–Fe5 86.8(2). In an exterior rhomb (Fe1N4Fe6N5): Fe1–N4 1.918(5), Fe1–N5 1.969(5), Fe6–N4 1.904(5), Fe6–N5 1.969(5), Fe1...Fe6 2.590(1), N4...N5 2.884(2); N4–Fe1–N5 95.8(2), N4–Fe6–N5 96.2(2), Fe1–N4–Fe6 85.3(2), Fe1–N5–Fe6 82.2(2).  $\angle$  = average.

graphically imposed inversion symmetry, but has nearly ideal noncrystallographic  $C_{4h}$  symmetry. It contains eight interior  $\mu_4$ -nitrogen atoms that are bound only to iron atoms, and four exterior  $\mu_3$ -nitrogen atoms that are each bound to the tin atom of one  $SnMe_3$  moiety and three iron atoms. The four independent  $\mu_4$ -nitrogen atoms (N1–N4) occupy butterfly-shaped ( $C_{2v}$  symmetry) environments, as exemplified by the angles  $Fe1-N1-Fe2 = 171.2(3)^\circ$  and  $Fe5-N1-Fe7 = 119.2(2)^\circ$ . The two independent  $\mu_3$ -nitrogen atoms (N5 and N6) occur in trigonal pyramidal  $SnNFe_3$  fragments. All iron atoms except  $Fe5/Fe5'$  occur in highly distorted tetrahedral  $Fe(\mu_3-N)(\mu_4-N)_2Cl$  units. The tin sites are more nearly tetrahedral.

The inner  $Fe_8N_8$  portion of the  $[Fe_{14}(\mu_4-N)_8(\mu_3-N)_4]^{4-}$  core may be described as a close-packed cube; the remaining  $Fe_6/Fe6'$  and  $N5/N5'$ , and  $Fe7/Fe7'$  and  $N6/N6'$  atoms are displaced outward from adjacent cube faces. The  $Fe_3N_4$  face defined by  $Fe1-Fe5$  and  $N1-N4$ , and its symmetry equivalent

are parallel and nearly planar. Within each of these  $\text{Fe}_5\text{N}_4$  faces, the atoms are connected into four edge-sharing  $\text{Fe}_2\text{N}_2$  rhombs. The  $\text{Fe}_4$  and  $\text{N}_4$  planes of each  $\text{Fe}_5\text{N}_4$  face are perfectly planar, and the dihedral angle between them is  $0.6^\circ$ .

The  $\text{Fe6/Fe6'}$ ,  $\text{Fe7/Fe7'}$ ,  $\text{N5/N5'}$ , and  $\text{N6/N6'}$  atoms define a nearly perfect  $\text{Fe}_4\text{N}_4$  plane, which is located between the two  $\text{Fe}_5\text{N}_4$  faces and extends beyond them to form the exterior of the cluster. The three planes are connected through four pairs of edge-sharing  $\text{Fe}_2\text{N}_2$  rhombs. As typical examples of the geometry, the dihedral angle between the planes of the exterior rhombs sharing an  $\text{Fe6-N5}$  edge is  $115.3^\circ$ , and the dihedral angle between the planes of the exterior and interior rhombs sharing an  $\text{Fe1-N4}$  edge is  $118.5^\circ$ . Thus, the cluster is built from 16  $\text{Fe}_2\text{N}_2$  rhombs.

The  $\text{Fe}_4\text{N}_2$  sides of the inner  $\text{Fe}_8\text{N}_8$  cube are also nearly planar and intersect at right angles. For example, the atom deviation from the  $\text{Fe}_4\text{N}_2$  plane defined by  $\text{Fe1}$ ,  $\text{Fe2}$ ,  $\text{Fe3'}$ ,  $\text{Fe4'}$ ,  $\text{N1}$ , and  $\text{N3'}$  is  $0.048 \text{ \AA}$ , and the dihedral angle between this plane and that defined by  $\text{Fe1'}$ ,  $\text{Fe2}$ ,  $\text{Fe3}$ ,  $\text{Fe4'}$ ,  $\text{N1}$ , and  $\text{N3'}$  is  $89.8^\circ$ . The  $\text{Fe6/Fe6'}$ ,  $\text{Fe7/Fe7'}$ ,  $\text{N5/N5'}$ , and  $\text{N6/N6'}$  atoms lie  $0.92\text{--}1.13 \text{ \AA}$  above the side  $\text{Fe}_4\text{N}_2$  planes.

The nexus of each  $\text{Fe}_5\text{N}_4$  face of the cluster is the  $\text{Fe5/Fe5'}$  site, which lies on the pseudo-fourfold axis. These iron atoms have square planar coordination environments, with an average  $\text{Fe}-(\mu_4\text{-N})$  distance of  $2.004(6) \text{ \AA}$  and an average  $\text{N-Fe-N}$  angle of  $89.7(3)^\circ$ . The  $\text{Fe5}$  atom deviates by  $0.224(1) \text{ \AA}$  from the  $\text{Fe}_4(1\text{--}4)\text{N}_4(1\text{--}4)$  plane of the face, and by  $0.158(3) \text{ \AA}$  from the  $\text{N}_4$  plane, in the direction of  $\text{Fe5'}$ . As a result, the  $\text{Fe5}\cdots\text{Fe5'}$  separation is  $2.783(2) \text{ \AA}$ ,  $0.58 \text{ \AA}$  shorter than the  $\text{Fe1}\cdots\text{Fe3'}$  distance of  $3.364(1) \text{ \AA}$  between the faces. The  $\text{N1}\cdots\text{N3'}$  distance between directly opposite nitrogen atoms is  $3.098(7) \text{ \AA}$ .

The  $\text{Fe}_2\text{N}_2$  rhomb emerges as the dominant structural feature of **3**. The dimensions of two typical rhombs are given in Figure 1. An apparent manifestation of the rigid connectivity of the fused rhomb core is the large departure from tetrahedral geometry at the iron sites. At the  $\text{Fe1}$  site, for example, the three  $\text{Cl-Fe-N}$  angles and the  $\text{N1-Fe1-N5}$  angle are in the range  $114.1(2)\text{--}116.3(2)^\circ$ , while the remaining  $\text{N1-Fe1-N4}$  and  $\text{N4-Fe1-N5}$  angles are constrained to  $95.8(2)^\circ$  by their inclusion in two different  $\text{Fe}_2\text{N}_2$  rhombs. The  $\text{Fe1-N1}$  and  $\text{Fe1-N4}$  bond lengths in the first rhomb average to  $1.91(2) \text{ \AA}$ , while the  $\text{Fe1-N5}$  distance in the second rhomb is  $1.969(5) \text{ \AA}$ . The same situation (but with different metric parameters) applies to the other tetrahedral iron sites.

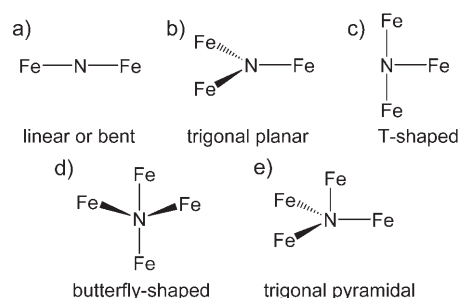
Likewise, the square planar geometry at the  $\text{Fe5}$  site is the result of rigid rhomb connectivity. It is probable that this site contains  $\text{Fe}^{\text{II}}$  ions, as the  $\text{Fe5-N}$  bond lengths are similar to the average  $\text{Fe}^{\text{II}}\text{-N}$  bond lengths in the complexes  $[\text{Fe}(\text{OEP})]$  ( $\text{OEP} = 2,3,7,8,12,13,17,18\text{-octaethylporphyrinato}$ ;  $2.00(2) \text{ \AA}$ ),<sup>[14]</sup>  $[\text{Fe}(\text{TPP})]$  ( $\text{TPP} = 5,10,15,20\text{-tetraphenylporphyrinato}$ ;  $1.966(2) \text{ \AA}$ ),<sup>[15]</sup> and  $[\text{Fe}(\text{OMP})]^{2-}$  ( $\text{OMP} = 5,5,10,10,15,15,20,20\text{-octamethylporphyrinogenato}$ ;  $1.93(1) \text{ \AA}$ ),<sup>[16]</sup> which all have square planar coordination geometries and  $S=1$  ground states. (Note that with the more flexible porphyrinogenato ligands, the  $\text{Fe}^{\text{II}}\text{-N}$  bond distances in square planar complexes are approximately  $0.04\text{--}0.05 \text{ \AA}$  longer than the  $\text{Fe}^{\text{III}}\text{-N}$  values.<sup>[16,17]</sup>) The mean  $\text{Fe-Cl}$  distance of  $2.240(9) \text{ \AA}$  within the 12  $\text{FeN}_3\text{Cl}$  fragments is

consistent with the expected value for an  $\text{Fe}^{\text{III}}$  ion in a (distorted) tetrahedral site, as judged by the  $\text{Fe}^{\text{III}}\text{-Cl}$  distances of  $2.24\text{--}2.27 \text{ \AA}$  in **1**<sup>[1]</sup> and of  $2.29\text{--}2.33 \text{ \AA}$  in salts of  $[\text{FeCl}_4]^{2-}$ .<sup>[18]</sup>

Initial magnetic measurements suggest an  $S=2$  ground state for **3**. At  $295 \text{ K}$ , the value of  $\chi_{\text{M}}T$  is  $5.89 \text{ cm}^3 \text{ K mol}^{-1}$  in an applied field of  $0.05 \text{ T}$ .  $\chi_{\text{M}}T$  remains nearly constant to  $115 \text{ K}$ , and decreases to  $4.80 \text{ cm}^3 \text{ K mol}^{-1}$  at  $5 \text{ K}$  (see Supporting Information). Variable-field magnetization data at  $2.0 \text{ K}$  reveal that the magnetization approaches saturation at a value of approximately  $4N\mu_{\text{B}}$  in a field of  $5 \text{ T}$ . The  $S=2$  ground state may arise from 12 antiferromagnetically coupled  $S=\frac{5}{2} \text{ Fe}^{\text{III}}$  ions that are additionally coupled to two  $S=1 \text{ Fe}^{\text{II}}$  ions. Accordingly, square planar  $\text{Fe}^{\text{II}}\text{N}_4$  complexes, such as those mentioned above and phthalocyaninatoiron(II),<sup>[19]</sup> usually have triplet ground states.

The Mössbauer spectrum of  $(\text{Et}_4\text{N})_4\text{3}$  at  $4.2 \text{ K}$  was fit under the assumption of a 6:1 site ratio: a doublet at an isomer shift of  $\delta = 0.38 \text{ mm s}^{-1}$  with a quadrupole splitting of  $\Delta E_{\text{Q}} = 0.77 \text{ mm s}^{-1}$  corresponds to the majority  $\text{Fe}^{\text{III}}$  ions, and a doublet at  $\delta = 0.48 \text{ mm s}^{-1}$  with  $\Delta E_{\text{Q}} = 2.11 \text{ mm s}^{-1}$  corresponds to the minority  $\text{Fe}^{\text{II}}$  ions (see Supporting Information). This fitting is compatible with the oxidation state assignment from the analysis of the magnetic data.

Several common features are emerging for iron nitride clusters. In structural terms, all of the clusters are built by the edge-sharing of  $\text{Fe}_2\text{N}_2$  rhombs. In binuclear and cluster iron nitride complexes, the five nitrogen-centered structural elements in Scheme 2 have been identified, and the coordi-



**Scheme 2.** Structural elements (idealized) found in iron nitride clusters with nuclearities of 2 (a), 4 (b), 10 (c–e), and 14 (d).

nation environment of the iron atoms in Scheme 2b–e is tetrahedral, square planar, or trigonal bipyramidal. The presence of  $\text{Fe}_2\text{N}_2$  rhombs is reminiscent of iron sulfide cluster chemistry, in which twelve structural types result from the edge- and/or vertex-sharing of  $\text{Fe}_2\text{S}_2$  rhombs.<sup>[20,21]</sup> Although three iron oxidation states (II, III, and IV) are found in iron nitride clusters, only two (II and III) are found in weak-field iron sulfide clusters. Lastly, in all of the binary iron nitride phases, except  $\text{FeN}$ , the atomic ratio of iron to nitrogen is greater than one, which is also the case in **1–3**. However, the structural elements noted here do not occur in  $\text{Fe}_2\text{N}$ ,  $\text{Fe}_3\text{N}$ ,  $\text{Fe}_4\text{N}$ , or  $\text{Fe}_{16}\text{N}_2$ .<sup>[22,23]</sup> The present work represents a further step in elucidating the synthetic and structural chemistry of iron nitride clusters.

## Experimental Section

All manipulations were carried out under a dinitrogen atmosphere in a glovebox. Anhydrous acetonitrile (Burdick & Jackson; < 10 ppm water) was dried over molecular sieves (4 Å). Diethylether and THF were distilled from sodium benzophenone ketyl and stored over molecular sieves (4 Å).

(Et<sub>4</sub>N)<sub>4</sub>3: A pale yellow solution of (Et<sub>4</sub>N)[FeCl<sub>4</sub>]<sup>[24]</sup> (0.33 g, 1.01 mmol) in acetonitrile (0.85 mL) was added to an emulsion of (Me<sub>3</sub>Sn)<sub>3</sub>N<sup>[25]</sup> (0.52 g, 1.02 mmol) in acetonitrile (0.85 mL). The black solution was stirred for 5 min and allowed to stand at room temperature for 11 h. The black mother liquor was decanted from black rectangular plates of other cluster products. The decanted solution was left standing for an additional 24 h, over which time large black truncated rhombohedra separated. The crystalline solid was collected by carefully decanting the mother liquor, washed with THF (5 × 3 mL) and ether (3 × 3 mL), and dried under vacuum to afford 0.033 g (18%) of product. Elemental analysis (%) calcd for C<sub>44</sub>H<sub>116</sub>Cl<sub>12</sub>Fe<sub>14</sub>N<sub>16</sub>Sn<sub>4</sub>: C 20.71, H 4.55, Cl 16.67, Fe 30.64, N 8.78, Sn 18.61; found: C 20.65, H 4.60, Cl 16.74, Fe 30.58, N 8.75, Sn 18.49.

Received: April 20, 2006

Published online: July 21, 2006

**Keywords:** cluster compounds · iron · nitrides · self-assembly · tin

Structures were solved by direct methods and refined against all data using SHELXTL 5.0. CCDC-604928 contains the supplementary crystallographic data for this paper. These data can be obtained free of charge from The Cambridge Crystallographic Data Centre via [www.ccdc.cam.ac.uk/data\\_request/cif](http://www.ccdc.cam.ac.uk/data_request/cif).

- [14] S. H. Strauss, M. E. Silver, K. M. Long, R. G. Thompson, R. A. Hudgens, K. Spartalian, J. A. Ibers, *J. Am. Chem. Soc.* **1985**, *107*, 4207–4215.
- [15] N. Li, Z. Su, P. Coppens, J. Landrum, *J. Am. Chem. Soc.* **1990**, *112*, 7294–7298.
- [16] J. Bachmann, D. G. Nocera, *J. Am. Chem. Soc.* **2005**, *127*, 4730–4743.
- [17] D. Jacoby, C. Floriani, A. Chiesi-Villa, C. Rizzoli, *J. Chem. Soc. Chem. Commun.* **1991**, 220–222.
- [18] J. W. Lauher, J. A. Ibers, *Inorg. Chem.* **1975**, *14*, 348–352.
- [19] C. G. Barraclough, R. L. Martin, S. Mitra, R. C. Sherwood, *J. Chem. Phys.* **1970**, *53*, 1643–1648.
- [20] R. H. Holm, in *Bio-coordination Chemistry, Vol. 8*, (Eds.: L. Que, Jr., W. A. Tolman), Elsevier, Oxford **2004**, pp. 61–90.
- [21] P. V. Rao, R. H. Holm, *Chem. Rev.* **2004**, *104*, 527–559.
- [22] H. Jacobs, D. Rechenbach, U. Zachwieja, *J. Alloys Compd.* **1995**, *227*, 10–17.
- [23] B. Eck, R. Dronskowski, M. Takahashi, S. Kikkawa, *J. Mater. Chem.* **1999**, *9*, 1527–1537.
- [24] N. S. Gill, *J. Chem. Soc.* **1961**, 3512–3515.
- [25] K. Sisido, S. Kozima, *J. Org. Chem.* **1964**, *29*, 907–909.

- [1] M. V. Bennett, S. Stoian, E. L. Bominaar, E. Münck, R. H. Holm, *J. Am. Chem. Soc.* **2005**, *127*, 12378–12386.
- [2] O. Einsle, F. A. Tezcan, S. L. A. Andrade, B. Schmid, M. Yoshida, J. B. Howard, D. C. Rees, *Science* **2002**, *297*, 1696–1700.
- [3] V. Vrajmasu, E. Münck, E. L. Bominaar, *Inorg. Chem.* **2003**, *42*, 5974–5988.
- [4] H.-I. Lee, P. M. C. Benton, M. Laryukhin, R. Y. Igarashi, D. R. Dean, L. C. Seefeldt, B. M. Hoffman, *J. Am. Chem. Soc.* **2003**, *125*, 5604–5605.
- [5] S. C. Lee, R. H. Holm, *Proc. Natl. Acad. Sci. USA* **2003**, *100*, 3595–3600.
- [6] T. Jüstel, T. Weyhermüller, E. Bill, M. Lengen, A. X. Trautwein, P. Hildebrandt, *Angew. Chem.* **1995**, *107*, 744; *Angew. Chem. Int. Ed. Engl.* **1995**, *34*, 669–672.
- [7] T. Jüstel, M. Müller, T. Weyhermüller, C. Kressl, E. Bill, P. Hildebrandt, M. Lengen, M. Grodzicki, A. X. Trautwein, B. Nuber, K. Wieghardt, *Chem. Eur. J.* **1999**, *5*, 793–810.
- [8] M. Li, M. Shang, N. Ehlinger, C. E. Schulz, W. R. Scheidt, *Inorg. Chem.* **2000**, *39*, 580–583.
- [9] T. A. Betley, J. C. Peters, *J. Am. Chem. Soc.* **2004**, *126*, 6252–6254.
- [10] S. D. Brown, J. C. Peters, *J. Am. Chem. Soc.* **2005**, *127*, 1913–1923.
- [11] R. Hourihane, T. R. Spalding, G. Ferguson, T. Deeney, P. Zanello, *J. Chem. Soc. Dalton Trans.* **1993**, 43–46.
- [12] R. Della Pergola, C. Bandini, F. Demartin, E. Diana, L. Garlaschelli, P. L. Stanghellini, P. Zanello, *J. Chem. Soc. Dalton Trans.* **1996**, 747–754.
- [13] Diffraction-quality crystals were obtained from the second crop collected from the mother liquor, as described above. Crystal data for (Et<sub>4</sub>N)<sub>4</sub>3·5 MeCN: C<sub>54</sub>H<sub>131</sub>Cl<sub>12</sub>Fe<sub>14</sub>N<sub>21</sub>Sn<sub>4</sub>, *M<sub>r</sub>* = 2756.91, *T* = 193 K, monoclinic, space group *C2/c*, *a* = 23.991(3), *b* = 18.450(3), *c* = 23.450(3) Å, β = 94.268(3)°, *V* = 10351(2) Å<sup>3</sup>, *Z* = 4, ρ<sub>calcd</sub> = 1.769 g cm<sup>-3</sup>, *R*<sub>1</sub> = 0.0584, *wR*<sub>2</sub> = 0.1140, 37311 reflections (12872 independent), 492 parameters, 0 restraints. Data were collected on a Bruker APEX diffractometer using graphite-monochromated MoK<sub>α</sub> (λ = 0.71073 Å) radiation, and were corrected for Lorentz, polarization, and absorption effects.